Space-charge waves in silicon carbide

M. P. Petrov, V. V. Bryksin, and A. A. Lebedev
Physico-Technical Institute, Russian Academy of Sciences, St. Petersburg 194021, Russia

M. Lemmer and M. Imlau[a)]
Department of Physics, University of Osnabrück, Barbarastrasse 7, D-49069 Osnabrück, Germany

(Received 5 July 2005; accepted 6 September 2005; published online 21 October 2005)

Space-charge waves (trap recharging waves) and the effect of spatial rectification of space-charge waves have been investigated in single crystals of 4*H*-SiC polytype. The relevant experimental dependencies have been found to be in quite good quantitative agreement with the theory of space-charge waves. The following parameters of the samples studied were determined: $\mu\tau = (7.4 \pm 0.8) \times 10^{-7}$ cm^2/V, $\tau_M = (5.3 \pm 0.6) \times 10^{-4}$ s, and $N_{\mathrm{eff}} = (5 \pm 1) \times 10^{13}$ cm^{-3}. © *2005 American Institute of Physics*. [DOI: 10.1063/1.2112180]

I. INTRODUCTION

Silicon carbide (SiC) is a wide-band-gap semiconductor which is of great interest for such applications as high-power semiconductor devices (thyristors and diodes), high-frequency electronics, and sensors operating in hostile environment and at high temperatures. Another very important area of applications is the use of these crystals as substrates for the fabrication of GaN-based devices emitting light in the green and blue spectral regions.[1,2] The investigation of space-charge waves (SCW) in SiC can be interesting for two reasons: The first one is the determination of the material parameters of the crystal under investigation, as SCW measurements provide information about the product of mobility, lifetime of the carriers ($\mu\tau$), the trap concentration (N_{eff}), the Maxwell relaxation time (τ_M), and others. The second reason is the investigation of the properties of SCW themselves, since this can be useful not only for a better understanding of the nature of SCW in semiconductors but also for the optimization of optical sensors detecting weak vibrations of various surfaces, for the development of devices for laser ultrasonic diagnostics, and for the optimization of specific photoreceivers.

SCW are eigenmodes of spatial-temporal oscillations of a space-charge density appearing in semi-insulating semiconductors in an external electric field.[3] For this paper we present investigations of the so-called low-frequency branch of SCW or (in other words) trap recharging waves. These waves are examples of the so-called backward waves where the dispersion law has an unusual shape (the eigenfrequency is inversely proportional to the wave number K) and, as a consequence, group and phase velocities are oriented in opposite directions. In the present paper we used an optical method for the excitation of SCW. The sample is illuminated by an oscillating interference pattern. For the detection of SCW we registered an alternating current arising in the sample due to the effect of spatial rectification of SCW.[4–6] Using this technique we detected resonance SCW excitation and investigated the position of the resonance and its signal amplitude at the resonance frequency as function of the applied field E_0, the K number of SCW, and the light intensity illuminating the crystal. A comparison of the obtained data with the developed theory allowed us to find $\mu\tau$, N_{eff}, and τ_M. Up to now investigations of SCW have mostly been performed in photorefractive crystals of the sillenite family.[7–10] Hence, there are only few papers devoted to the SCW investigations in classical semiconductors (e.g., Ref. 11).

II. DESCRIPTION OF THE SAMPLE AND EXPERIMENTAL SETUP

In the experiments a single crystal of the 4*H*-SiC polytype was used (a hexagonal unit cell with a wurtzite structure). The size of the sample was $6.5 \times 8 \times 0.45$ mm^3. The c axis is perpendicular to the surface (6.5×8 mm^2) illuminated by the oscillating fringe pattern. The electric field was applied via two metallic (Ni) electrodes deposited by magnetron sputtering on the surface of the sample, so that the electric field was normal to the c axis. The distance between the electrodes was approximately 5 mm. The configuration of the experimental setup is shown in Fig. 1(a). An Ar$^+$-ion laser was used as a source of coherent light ($\lambda = 488$ nm, output power of 2 W). The adjustment of the light intensity was accomplished by a combination of a half-wave retarder plate and a polarizer. The expanded light beam was split into two arms to form an interferometer. The phase of the light in one of the beams was modulated by a phase modulator. Two beams incident upon the surface of the sample and form a light intensity interference pattern $W(x,t)$. The interference pattern is given by

$$W(x,t) = W_0[1 + m\cos(Kx + \Theta\cos\Omega t)]$$
$$\cong W_0 + W_0 m\cos Kx - \frac{W_0 m\Theta}{2}\sin(Kx - \Omega t)$$
$$- \frac{W_0 m\theta}{2}\sin(Kx + \Omega t). \qquad (1)$$

Here, W_0 is the average light intensity, m is the contrast ratio of the interference pattern, $K = 2\pi/\Lambda$ is the wave number of the interference pattern, $\Lambda = \lambda/(2\sin\phi)$ is the grating spac-

[a)]Electronic mail: mirco.imlau@uni-osnabrueck.de

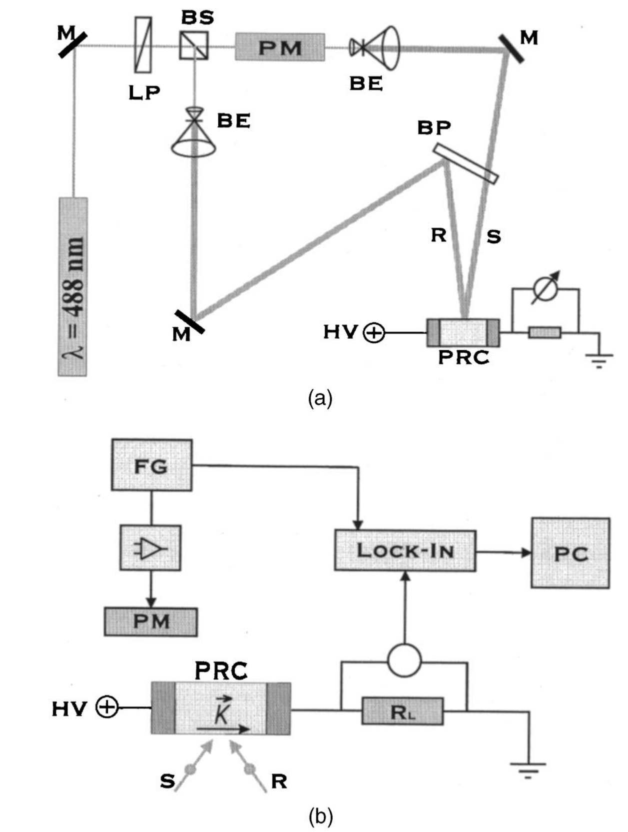

FIG. 1. (a) Experimental setup (schematically); LP is a combination of a half-wave plate and a polarizer, BS is a beam splitter, PM is a phase modulator, BE is a beam expander, M is a mirror, and PRC is a studied crystal. An argon-ion laser at $\lambda = 488$ nm with an output power of 2.0 W ($W_0 = 106$ mW/cm^2) was used. (b) Diagram demonstrating the electronic detection of SCW; HV is a high-voltage source, R_L is a loading resistor, and FG is a function generator.

ing, ϕ is the angle of incidence of the illuminating beams (a symmetrical geometry of the illumination of the crystal is supposed), θ is the phase modulation amplitude, and $\Omega = 2\pi f$, where f is the frequency of the phase modulation. In Eq. (1) we assumed that $\Theta \ll 1$, so any term with a higher order of Θ is ignored. However, it has been experimentally verified that Eq. (1) can be used for the description of the experiments, even for the interval $0 < \Theta \leq 1$. The incident light excites photocarriers (electrons in our case) in accordance with the interference pattern of Eq. (1) resulting in several charge gratings. Some of them are gratings of free carriers and others are gratings of ionized traps. The charge grating that is proportional to $W_0 m \cos(Kx)$ is a static one, whereas the charge gratings proportional to $\sin(Kx - \Omega t)$ and $\sin(Kx + \Omega t)$ are running gratings moving in opposite directions. When the direction of propagation as well as the K value and Ω of one of the running gratings coincide with the direction of propagation, wave number, and eigenfrequency of one of the eigenmodes of SCW, this mode of SCW experiences a resonance excitation. As the excited space-charge wave propagates along the static grating, a current—alternating in time but homogeneous in space—arises due to the interaction between the moving periodical charge density and the static periodical field of the static grating. The moving charge density contains phase multipliers of the form $\exp(Kx - \Omega t)$ and the static space-charge field grating contains multipliers of the form $\exp(-Kx)$. Since the current is proportional to the product $\exp(Kx - \Omega t)\exp(-Kx) = \exp(-\Omega t)$, it does not depend on the coordinate but it oscillates in time. This current can be detected in the outside circuit [see Fig. 1(b)]. In the experiment, we placed a loading resistor (with a much lower resistance than that of the sample) in series with the crystal, so that in our case the output signal was an ac voltage on the loading resistor. This signal was then amplified by a lock-in amplifier and finally data were stored in a computer.

III. THEORETICAL BACKGROUND

The general theory of SCW and the effect of spatial rectification of SCW has been developed in detail[4–6] for a number of most important specific situations. However, in the published papers,[4–6] where the effect of SCW rectification was analyzed, the effect of trap saturation was not taken into account because the trap density in the materials studied was high enough. In this paper we perform similar calculations,[6] but we take a limited trap density in SiC into account. The details of our calculations will be published elsewhere. Here we present the expressions for the frequency dependence of the output signal real amplitude $I_1(\Omega)$ and the expression for the frequency position (Ω_R) of the signal maximum.

The expression for the modulus of the output signal amplitude is

$$I_1(\Omega) = \frac{\sigma E_0 m^2 \Theta \Omega \tau_M d}{2\{(\Omega \tau_M d - 1)^2 + [\Omega \tau_M + (E_0/E_q)]^2\}^{1/2}(\Omega \tau_M d + 1)}. \tag{2}$$

Here, $d = \mu\tau E_0 K$, μ is the carrier mobility, τ is the carrier lifetime, E_0 is the applied electric field in the crystal, $E_q = eN_{\text{eff}}/(\epsilon\epsilon_0 K)$, N_{eff} is the effective trap concentration, ϵ is the relative dielectric constant of the crystal, and e is the charge of an electron. Equation (2) is obtained under the conditions $d \gg 1$, $E_0/E_q \ll 1$, arbitrary dE_0/E_q, and the absence of screening effects that reduce the internal electric field. Note that in many cases the screening effects in sillenites play a very important role. However, in SiC we did not observe any experimental indications of screening effects and, therefore, these effects were not taken into account in our calculations. In Eq. (2) we ignored diffusion effects as the applied electric field was much higher than the so-called diffusion field at any K used. More general theoretical calculations will be published elsewhere.

As can be seen from Eq. (2), the signal amplitude exhibits a maximum which indicates (under definite conditions) that SCW are excited. The maximum occurs at frequency

$$\Omega_R = \frac{1}{\tau_M \sqrt{(d^2 + 1)}}. \tag{3}$$

This expression is correct not only for $d \gg 1$ but also for $d \approx 1$. Note that in the case $d \gg 1$ the maximum of the signal corresponds to the resonance excitation of SCW, and the resonance frequency is then given by

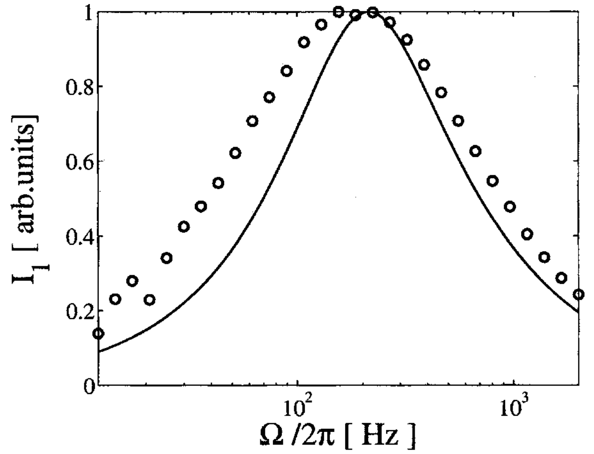

FIG. 2. Frequency dependence of the ac current amplitude $I_1(\Omega)$ (which is proportional to the SCW amplitude) for W_0=106 mW/cm^2, K=10^3 cm^{-1}, E_0=1.5 kV/cm, Θ=0.62, and m=0.5. The circles (○) are experimental values and the solid line is the theoretical calculation in accordance with Eq. (2). Here, and in what follows, the fitting parameters mentioned in the text were used to calculate the theoretical curves.

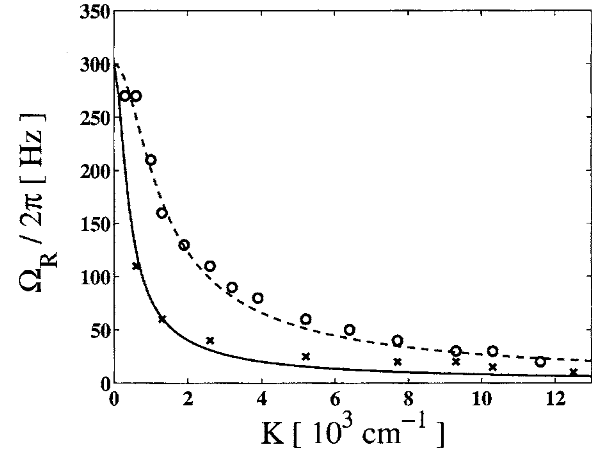

FIG. 3. Resonance frequency as a function of the wave number K for W_0 =106 mW/cm^2, Θ=0.62, m=0.5, and two different values of the applied electric field E_0. The circles (○) are experimental values for E_0 =1.5 kV/cm and the crosses (×) are experimental values for E_0 =5.0 kV/cm. The solid lines are theoretical calculations in accordance with Eq. (3).

$$\Omega_R \approx \frac{1}{\tau_M \tau_\mu K E_0}. \quad (4)$$

Equation (4) coincides with the dispersion law of trap recharging waves.[3] However, at $d<1$ the maximum of the output signal means that a maximum of the current arises due to the competition between the two components of the current propagating in opposite directions. These two components correspond to the resonant and nonresonant terms of running gratings in Eq. (1). At $d<1$, both components correspond to the excitation of relaxation oscillations rather than to the excitation of SCW. Under the conditions which are quite typical of the SiC sample studied ($d \gg 1$, $E_0/E_q<1$, and $dE_0/E_q>1$) the signal amplitude at the resonance maximum is

$$I_1(\Omega_R) \approx \frac{\sigma E_0 m^2 \Theta_M d}{4[1+(dE_0/E_q)]} \propto \frac{E_0^2 K}{1+(\epsilon\epsilon_0 \mu\tau E_0^2 K^2/eN_{\text{eff}})}. \quad (5)$$

It follows from Eq. (5) that the dependence of the output signal on K may have a maximum that allows us to estimate the trap concentration N_{eff}.

IV. EXPERIMENTAL RESULTS

Figure 2 shows one example of the output signal amplitude (in arbitrary units) as a function of the phase modulation frequency. The resonance character of the frequency dependence clearly points to the resonance character of SCW excitation. The solid curve corresponds to the theoretical calculation in accordance with Eq. (2). One can see a reasonable agreement between theory and experiment. Here the following fitting parameters were used: $\mu\tau$=(7.4±0.8) $\times 10^{-7}$ cm^2/V, τ_M=(5.3±0.6)$\times 10^{-4}$ s, and N_{eff}=(5±1) $\times 10^{13}$ cm^{-3}. The value of $\epsilon \approx 10$ (Refs. 2 and 12) was used to calculate N_{eff}. The same fitting parameters will be used for all theoretical curves in the figures below. Figure 3 shows the dependence of the position of the signal maximum on the wave number K for two different values of the applied electric field. Figure 4 shows the dependence of the signal maximum position on the applied electric field. Figures 3 and 4 provide the proof that the detected resonance is due to excitation of SCW as resonance frequencies coincide with the dispersion law for the considered SCW for the case $d \gg 1$.

Figure 5 shows the dependence of the signal amplitude at the resonance on K for two different values of E_0. In the case E_0=1.5 KV/cm a pronounced maximum appears at $K \approx 2\times 10^3$ cm^{-1}. This dependence allows us to determine the trap density N_{eff}.

Figure 6 shows the dependence of the signal amplitude on the applied field E_0. One can see a quite reasonable agreement with the theory [relationship Eq. (5)]. Figure 7 shows the signal intensity and the resonance frequency as functions of the average light intensity illuminating the crystal. Since we deal with a photoconductor, the conductivity is given by

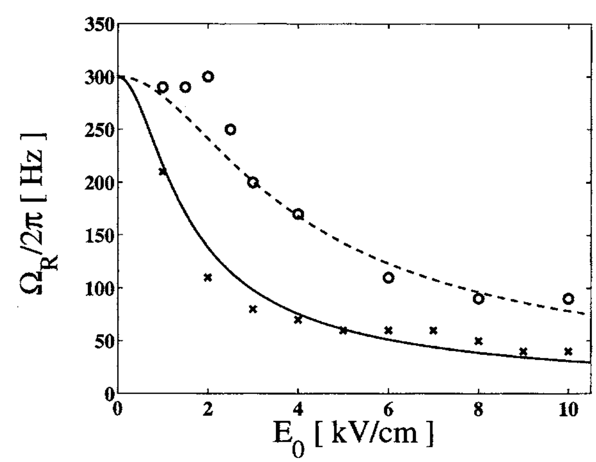

FIG. 4. Resonance frequency as a function of the applied electric field E_0 for W_0=106 mW/cm^2, Θ=0.62, m=0.5, and two different values of the wave number K. The circles (○) are experimental values for K=0.5 $\times 10^3$ cm^{-1} and the crosses (×) are experimental values for K=1.3 $\times 10^3$ cm^{-1}. The solid lines are theoretical calculations in accordance with Eq. (3).

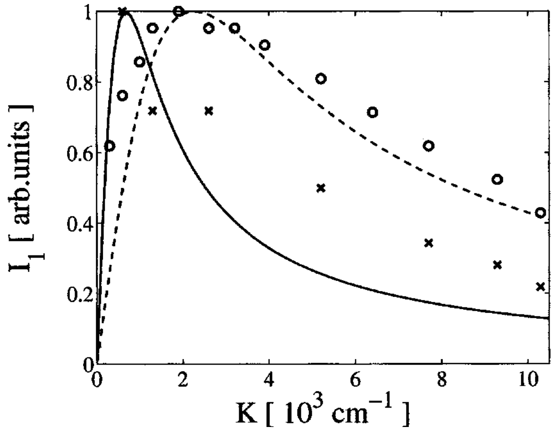

FIG. 5. Dependence of the amplitude at resonance on the wave number K for $W_0=106\ \mathrm{mW/cm^2}$, $\Theta=0.62$, $m=0.5$, and two different values of the applied electric field E_0. The circles (○) are experimental values for $E_0=1.5\ \mathrm{kV/cm}$ and the crosses (×) are experimental values for $E_0=5.0\ \mathrm{kV/cm}$. The solid lines are theoretical calculations in accordance with Eq. (5).

$$\sigma=\sigma_d+\sigma_{\mathrm{ph}}=\sigma_d+\frac{\alpha\beta W_0 e\mu\tau}{h\omega} \tag{6}$$

Here, σ_d is the dark conductivity, α is the light absorption coefficient, β is the quantum efficiency of the photoactive centers, and $\hbar\omega$ is the photon energy. In our case $\sigma_d \ll \sigma_{\mathrm{ph}}$, so in accordance with Eqs. (3) and (5) the signal amplitude must be proportional to the light intensity. This conclusion corresponds with the experimental results. At the same time the Maxwell relaxation time is expressed by $\tau_M=\epsilon\epsilon_0/\sigma$. Then it follows from Eqs. (4) and (6) that the resonance frequency must be proportional to W_0, which is also in agreement with the experimental results. We further performed measurements of the signal amplitude as a function of Θ and contrast ratio m. It has been found that the signal is proportional to Θ up to $\Theta=0.9$ rad and to m^2 up to $m=0.6$. This is in good agreement with the relationships in Eqs. (3) and (5).

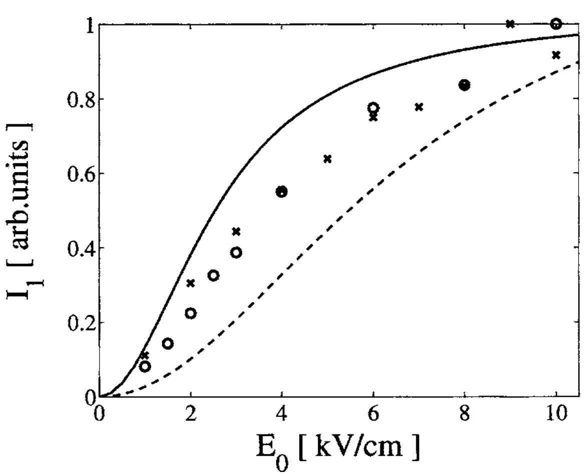

FIG. 6. Dependence of the amplitude at resonance on the applied electric field E_0 for $W_0=106\ \mathrm{mW/cm^2}$, $\Theta=0.62$, $m=0.5$, and two different values of the wave number K. The circles (○) are experimental values for $K=0.5\times10^3\ \mathrm{cm^{-1}}$ and the crosses (×) are experimental values for $K=1.3\times10^3\ \mathrm{cm^{-1}}$. The solid lines are theoretical calculations in accordance with Eq. (5).

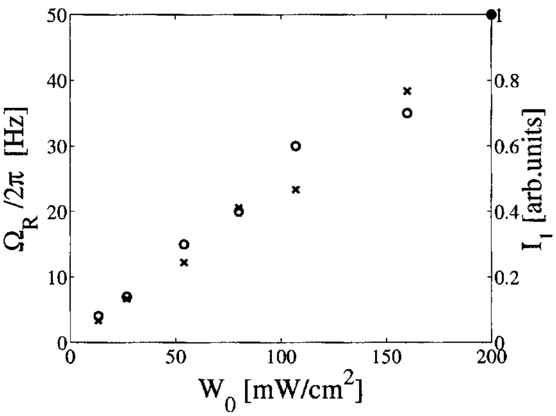

FIG. 7. Dependence of resonance frequency (○) and the amplitude (×) on the average light intensity W_0 for $K=10^3\ \mathrm{cm^{-1}}$, $E_0=5.0\ \mathrm{kV/cm}$, $\Theta=0.62$, and $m=0.5$.

V. DISCUSSION

The quite good agreement between the experimental and theoretical data proves unambiguously that the observed effects are associated with the excitation of trap recharging waves and with the effect of spatial rectification of these waves. The fitting parameters τ_M and $\mu\tau$ give quite reasonable values. The Maxwell relaxation time τ_M can be determined from the relationship $\tau_M=\epsilon\epsilon_0/\sigma$, too (when the magnitude of σ is determined from direct measurements of the current). From this estimation it follows that $\tau_M=1.6\times10^{-4}$ s. It correlates with $\tau_M=5.3\times10^{-4}$ s determined from SCW measurements. However, the value of the effective trap concentration N_{eff} seems to be very low. Let us discuss this question in more detail. The formula $E_q=eN_{\mathrm{eff}}/\epsilon\epsilon_0K$ mentioned above was obtained in the scope of a traditional simplest monopolar model of the formation of a space-charge distribution in semi-insulating crystals.[7,12] In accordance with this model, the crystal contains two kinds of the centers with energy levels somewhere in the band gap of the crystal. The first kind of the centers is a donor with concentration N_D (it is a sum of neutral donors and positively ionized donors with concentration N_D^+), and the second kind of the centers is a negatively ionized acceptor with concentration N_A^-. The condition that the homogeneous part of N_D^+ (in darkness) is equal to N_A^- is assumed. In the case when the incident light interference pattern excites electrons from the neutral donors, a spatially periodical variation of the space charge is associated with a periodical variation of N_D^+. The ratio between the nonhomogeneous and the homogeneous parts of N_D^+ is proportional to m but is much less than m, as the number of photoexcited electrons is much less than N_D^+ (this assumption agrees with the experimental fact that the photoconductivity is linearly proportional to the light intensity). In this model it is assumed that only one trap level (donors) is active whereas the acceptors are present only to ensure the overall charge neutrality. In accordance with the described model, N_{eff} is determined as follows:

$$N_{\mathrm{eff}}=N_A^-(1-N_A^-/N_D)=N_D^+(1-N_D^+/N_D). \tag{7}$$

The same model is valid, if the photoconductivity is determined by photoexcited holes. In this case the energetic positions of donor and acceptor are changed, but the final relationship for N_{eff} is the same. In many cases (in sillenites, for instance) $N_A^-/N_D \ll 1$ and N_{eff} means the concentration of ionized donors or acceptors. However, the trap concentration in our sample of SiC measured by deep level transient spectroscopy[13] (DLTS) is of the order of $10^{15}-10^{16}\ \mathrm{cm}^{-3}$, which is two orders of magnitude higher than N_{eff} calculated from our experimental data. There are several interpretations of N_{eff}. One possibility (it is likely that it is more probable) is that N_{eff} is the number of ionized donors. Note that in special cases (but it is not our case) it can be equal to the number of electrons in the conduction band. Another possibility is that N_A^-/N_D is of the order of unity, which also explains a low value of N_{eff}. The condition $N_A^-/N_D \approx 1$ means that $N_{\mathrm{eff}} \approx N_D - N_D^+$, i.e., the effective number of traps is equal to the number of neutral donors, and the phenomenon of trap saturation is associated with a shortage of neutral donors. Of course, the low value of N_{eff} can be explained in other ways as well. A monopolar two species model (the model with at least two active levels) and a bipolar model, or "one-species electron-hole competition model" (with only one active level, like in the monopolar model), but with two kinds (electrons and holes) of photoexcited carriers can be used. In principle, even a more complicated bipolar model with two active levels can also be invoked (a comprehensive review of the papers devoted to various models of the space-charge grating formation can be found in Ref. 7). In any of these more complicated models (including the formation of gratings of positive and negative charges), the space-charge fields of the gratings partially (or even completely in definite cases) compensate each other, which results in a weak net electric field grating, which can also be described by a corresponding N_{eff}. However, verification of different complicated models requires complementary experimental data.

VI. CONCLUSIONS

The investigation of trap recharging space-charge waves and the effect of SCW spatial rectification has been performed in the 4*H*-SiC polytype. The relevant experimental dependencies, in particular, the dispersion law of SCW, are in quite good quantitative agreement with the theory of SCW. The dependences of the amplitude of the oscillating current, caused by the effect of SCW rectification on the wave number of SCW and applied electric field, are described theoretically quite well with the following fitting parameters: $\mu\tau = (7.4 \pm 0.8) \times 10^{-7}\ \mathrm{cm}^2/\mathrm{V}$, $\tau_M = (5.3 \pm 0.6) \times 10^{-4}$ s, and $N_{\mathrm{eff}} = (5 \pm 1) \times 10^{13}\ \mathrm{cm}^{-3}$.

ACKNOWLEDGMENTS

Financial support from the Presidium of Russian Academy of Sciences (Program P-28) and the Deutsche Forschungsgemeinschaft (Project Nos. GRK 695 and 436 RUS 17/11/05) is gratefully acknowledged.

[1] P. Mandracci, G. Fanchini, S. Ferrero, C. Ricciardi, and L. Scaltrito, *Recent Research Developments in Applied Physics* (Transworld Research Network, Kerala, India, 2003), Vol. 6, Part II, pp. 427–450.
[2] *Properties of Advanced semiconductor Materials: GaN, AlN, InN, BN, SiC, SiGe*, edited by M. E. Levinshtein, S. L. Rumyantsev, and M. S. Shur (Wiley, New York, 2001).
[3] R. F. Kazarinov, R. A. Suris, and B. I. Fuks, Sov. Phys. Semicond. **6**, 500 (1972).
[4] S. Mansurova, S. Stepanov, N. Korneev, and C. Dibon, Opt. Commun. **152**, 207 (1998).
[5] M. P. Petrov, V. V. Bryksin, F. Rahe, C. E. Rueter, and E. Kraetzig, Opt. Commun. **227**, 183 (2003).
[6] V. V. Bryksin, P. Kleinert, and M. P. Petrov, Phys. Solid State **45**, 2044 (2003).
[7] L. Solymar, D. J. Webb, and A. Grunnet-Jepsen, *The Physics and Applications of Photorefractive Materials*, Oxford Series on Optical and Imaging Sciences Vol. 11 (Oxford University Press, New York, 1996).
[8] H. C. Pedersen, D. J. Webb, and P. M. Johansen, J. Opt. Soc. Am. B **15**, 2573 (1998).
[9] V. V. Bryksin and M. P. Petrov, Phys. Solid State **44**, 1869 (2002).
[10] M. Bryushinin, V. Kulikov, and I. Sokolov, Phys. Rev. B **67**, 075202 (2003).
[11] M. P. Petrov, V. V. Bryksin, C. E. Rueter, F. Rahe, A. Emgrunt, M. Imlau, and E. Kraetzig, Phys. Rev. B **69**, 241201(R) (2004).
[12] N. V. Kukhtarev, V. B. Markov, S. G. Odulov, M. S. Soskin, and V. L. Vinetskii, Ferroelectrics **22**, 949 (1979).
[13] A. A. Lebedev, Semiconductors **33**, 107 (1999).